

Polarized Raman spectra in GaN

This article has been downloaded from IOPscience. Please scroll down to see the full text article.

1995 J. Phys.: Condens. Matter 7 L129

(<http://iopscience.iop.org/0953-8984/7/10/002>)

View [the table of contents for this issue](#), or go to the [journal homepage](#) for more

Download details:

IP Address: 171.66.16.179

The article was downloaded on 13/05/2010 at 12:41

Please note that [terms and conditions apply](#).

LETTER TO THE EDITOR

Polarized Raman spectra in GaN

T Azuhata†, T Sota†‡, K Suzuki†§ and S Nakamura||

† Department of Electrical Engineering, Waseda University, Shinjuku, Tokyo 169, Japan

‡ Advanced Research Centre for Science and Engineering, Waseda University, Shinjuku, Tokyo 169, Japan

§ Kagami Memorial Laboratory for Material Science and Technology, Waseda University, Shinjuku, Tokyo 169, Japan

|| Department of Research and Development, Nichia Chemical Industries Ltd, 491 Oka, Kaminaka, Anan, Tokushima 774, Japan

Received 28 November 1994

Abstract. We have measured polarized Raman spectra in a 2.0 μm GaN epitaxial layer of high quality, grown on a sapphire substrate. All symmetry-allowed optical phonons in GaN have been assigned as follows: $A_1(\text{LO})$, 735 cm^{-1} ; $A_1(\text{TO})$, 533 cm^{-1} ; $E_1(\text{LO})$, 743 cm^{-1} ; $E_1(\text{TO})$, 561 cm^{-1} ; E_2 , 144 and 569 cm^{-1} . Using the Lyddane–Sachs–Teller relation, the static dielectric constants of GaN for the ordinary and extraordinary directions have been estimated as $\epsilon_{\perp 0} = 9.28$ and $\epsilon_{\parallel 0} = 10.1$. We have also observed quasi-LO phonons in GaN. A brief discussion on these will be given.

The III–V nitrides are considered as promising materials for optical device application in the blue and ultraviolet wavelength region [1]. However, as is well known, it has been difficult to grow high-quality films. Furthermore, obtaining p-type films has been a problem for a long time. Quite recently the difficulty has been overcome and the double-heterostructure light-emitting diode, whose structure is p-AlGaIn/GaN:Zn/n-AlGaIn and where the output power is about 1.5 mW, has been put to practical use by one of us (SN) [2–6].

Phonon modes of GaN have received considerable attention because information on them is important in considering the electron transport, the non-radiative electron relaxation process, and so on. In most of the Raman scattering measurements performed for GaN to date [7–12] similar phonon frequencies have been observed in spite of the sample quality varying from sample to sample. However, there has not been any work in which all symmetry-allowed optical phonons are detected in only one sample according to the polarization selection rules. We have succeeded in determining all of the Raman-active phonon frequencies using a high-quality single-crystal GaN film grown on a sapphire substrate. We have also observed quasi-longitudinal optical (LO) phonons in GaN, which are mixed modes of $A_1(\text{LO})$ and $E_1(\text{LO})$.

The sample used in this letter was grown on a sapphire (0001) substrate by the two-flow MOCVD method. Details of the two-flow MOCVD technique have been described in [2]. The sample structure was $\text{In}_{0.05}\text{Ga}_{0.95}\text{N}/\text{GaN}/\text{sapphire}$ substrate. The target values for the thickness of each layer were 0.05 μm and 2 μm for InGaIn and GaN, respectively. The InGaIn layer was doped with about 5×10^{19} Si cm^{-3} . The as-grown sample had an optically flat surface. The quality of the sample was the same as that of the double-heterostructure light-emitting diode [5, 6]. Note that the InGaIn top layer is too thin for us to detect phonons in InGaIn.

In our sample, GaN crystallizes in a wurtzite structure whose Z -axis is perpendicular to the sapphire substrate plane. The space group is C_{6v}^4 . Two formula units are contained in the unit cell. According to the factor group analysis at the Γ point, optical phonons belong to the following irreducible representations:

$$\Gamma_{\text{opt}} = A_1(Z) + 2B + E_1(X, Y) + 2E_2$$

where the X , Y , and Z in parentheses represent the polarization directions. Raman-active phonons belong to $A_1(Z)$, $E_1(X, Y)$, and E_2 modes and infrared-active ones to $A_1(Z)$ and $E_1(X, Y)$ modes. B modes are silent. Taking account of the sample orientation and the Raman tensor for C_{6v}^4 , we may observe all symmetry-allowed phonons in the configurations, for example, listed in table 1. Here $X \parallel [100]$, $Y \parallel [010]$, $Z \parallel [001]$, $A = (\sin \theta, -\cos \theta, 0)$, and $B = (\cos \theta, \sin \theta, 0)$ with $\theta \approx 108^\circ$.

Table 1. Scattering configurations and observable modes for wurtzite GaN. $X \parallel [100]$, $Y \parallel [010]$, $Z \parallel [001]$, $A = (\sin \theta, -\cos \theta, 0)$, and $B = (\cos \theta, \sin \theta, 0)$ with $\theta = 108^\circ$.

Scattering configuration	Mode
$Y(XX)\bar{Y}$	$A_1(\text{TO})$ and E_2
$Y(ZZ)\bar{Y}$	$A_1(\text{TO})$
$Y(ZX)\bar{Y}$	$E_1(\text{TO})$
$Z(XY)\bar{Z}$	E_2
$Z(XX)\bar{Z}$	$A_1(\text{LO})$ and E_2
$A(ZX)Y$	$E_1(\text{TO})$ and $E_1(\text{LO})$
$A(ZZ)Y$	$A_1(\text{TO})$
$A(BX)Y$	$A_1(\text{TO})$ and E_2

Raman spectra were recorded at room temperature. Second harmonics, $\lambda_L = 532 \text{ nm}$ ($E_L = 2.33 \text{ eV}$), of a quasi-CW $\text{Nd}^{3+}:\text{YAG}$ laser were used as an exciting light source. The incident laser power was $I_L \sim 100 \text{ mW}$. The scattered light was dispersed by a triple 1.0 m focal length spectrograph, which consists of a double subtractive filter and a spectrograph stage, and detected by an image-intensified multichannel detector. To avoid Raman scattering from air in the low-frequency region, the sample was mounted in vacuum if necessary. In analysing spectra, Lorentzian and/or Gaussian fits were performed and each peak position was determined.

In figure 1 Raman spectra for the configurations $Y(XX)\bar{Y}$, $Y(ZZ)\bar{Y}$, and $Y(ZX)\bar{Y}$ are shown. The observable sapphire modes are $A_{1g} + E_g$, A_{1g} , and E_g for the first, second, and third configurations respectively, where the phonon frequencies of sapphire are 418 and 645 cm^{-1} for A_{1g} and 378, 432, 451, 578 and 751 cm^{-1} for E_g [13]. The $Y(XX)\bar{Y}$ spectra clearly show 144 and 569 cm^{-1} E_2 modes as expected from the polarization selection rules shown in table 1. We assign the 533 cm^{-1} peak in the $Y(ZZ)\bar{Y}$ spectra to an A_1 transverse optical (TO) mode in accordance with table 1. This mode also appears in the $Y(XX)\bar{Y}$ spectra. The 561 cm^{-1} peak in the $Y(ZX)\bar{Y}$ spectra is assigned to $E_1(\text{TO})$. A leakage of $A_1(\text{TO})$ and E_2 modes is seen in the same spectra. A peak labelled QLD appears in the $Y(ZZ)\bar{Y}$ spectra. This is not due to sapphire and the origin will be discussed below.

Figure 2 shows Raman spectra for the configurations $Z(XY)\bar{Z}$ and $Z(XX)\bar{Z}$ in the range from 650 cm^{-1} to 850 cm^{-1} . The 750 cm^{-1} peak corresponds to one of the E_g modes in sapphire [13]. The peak at 735 cm^{-1} , which appears clearly in the $Z(XX)\bar{Z}$ configuration and disappears in the $Z(XY)\bar{Z}$ spectra, is assigned to an $A_1(\text{LO})$ mode conformably with table 1.

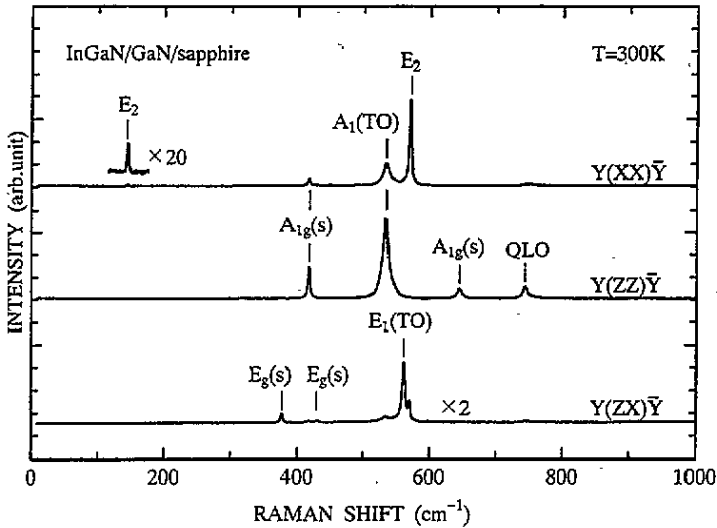


Figure 1. Polarized Raman spectra for the configurations $Y(XX)\bar{Y}$, $Y(ZZ)\bar{Y}$, and $Y(ZX)\bar{Y}$. $A_g(s)$ and $E_g(s)$ represent A_g and E_g modes of sapphire, respectively. As regards the peaks labelled QLO, see the text.

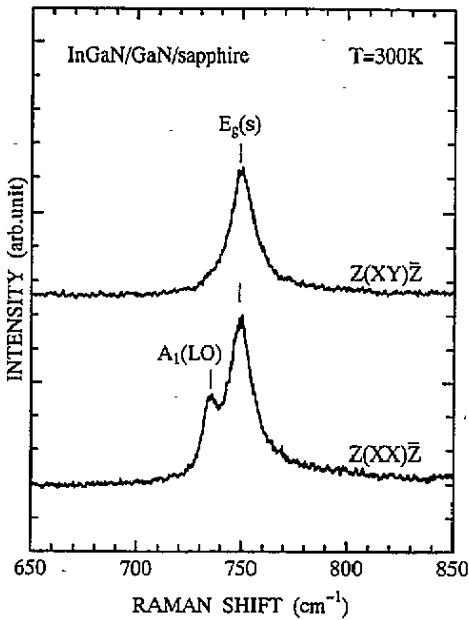


Figure 2. Polarized Raman spectra for the configurations $Z(XY)\bar{Z}$ and $Z(XX)\bar{Z}$. $E_g(s)$ denotes an E_g mode of sapphire.

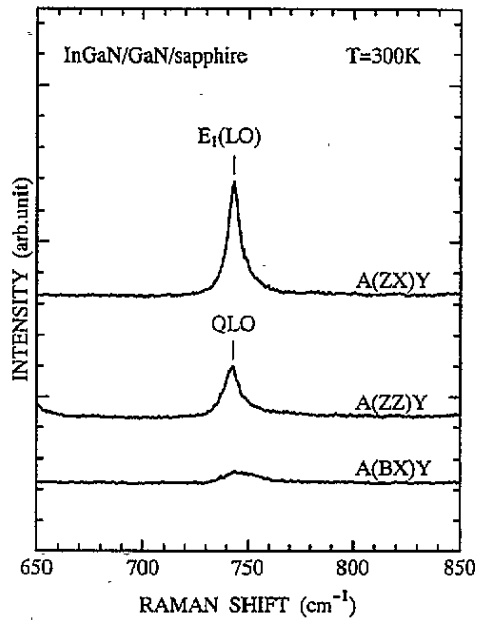


Figure 3. Polarized Raman spectra for the configurations $A(ZX)Y$, $A(ZZ)Y$, and $A(BX)Y$. For the notation A and B , and the peak labelled QLO, see the text.

In figure 3 Raman spectra measured in the quasi-right-angle scattering configurations $A(ZX)Y$, $A(ZZ)Y$, and $A(BX)Y$ are shown. According to table 1, $E_t(LO)$ and $E_t(TO)$ are allowed in the configuration $A(ZX)Y$. Thus the 743 cm^{-1} peak is assigned to $E_t(LO)$. As predicted by the polarization selection rules this mode does indeed disappear in the

configuration $A(BX)Y$. Table 1 shows that only $A_1(\text{TO})$, which is at 533 cm^{-1} , is allowed in the configuration $A(\text{ZZ})Y$ but a peak with moderate strength is found at 742 cm^{-1} as shown in figure 3. This is not due to sapphire and its frequency is slightly lower than that of $E_1(\text{LO})$.

Table 2. Phonon frequencies in wurtzite GaN obtained by Raman spectroscopy at room temperature. For comparison, results from previous work are also shown.

Mode	Phonon frequency (cm^{-1})						Present work
	[7]	[8]	[9] ^a	[10]	[11]	[12]	
A_1	LO	—	—	710	—	—	735
	TO	533	533	533	—	534	533
E_1	LO	—	—	741	—	—	743
	TO	559	559	559	—	—	561
E_2		568	568	568	568	568	569
		145	—	143	—	—	144

^a Two kinds of sample, i.e. needles and epitaxial films grown on sapphire substrates, were used.

^b To be precise, this is a frequency of a quasi-LO mode. See the text.

The phonon frequencies obtained herein are summarized in table 2, where previous results determined by the use of Raman spectroscopy are also shown for comparison. With respect to an $A_1(\text{LO})$ mode our frequency is 25 cm^{-1} higher than that of [9]. This discrepancy may be mainly due to the sample quality differences. As for the other modes, our values are consistent with the previous ones. Our results for $A_1(\text{LO})$, $A_1(\text{TO})$, $E_1(\text{LO})$, and $E_1(\text{TO})$ are also consistent with those obtained from infrared measurements [7, 14]. We have performed measurements of infrared reflectivity and attenuated total reflection with circularly polarized light and analysed the spectra using a classical oscillator model, though they are not shown here. The results are consistent with the present Raman results.

We consider the origin of two peaks labelled QLO, appearing in the configurations $Y(\text{ZZ})\bar{Y}$ and $A(\text{ZZ})Y$ where $A \approx Z$. Argüello *et al* [15] developed the theory of the first-order Raman effect in wurtzite-type crystals where the electrostatic forces dominate over the anisotropy in the short-range forces—in other words, the LO–TO splitting is much greater than the A_1 – E_1 splitting. According to the theory, A_1 and E_1 modes are mixed to become quasi-LO, quasi-TO, and pure TO modes except when phonons propagate parallel to the XY -plane or to the Z -axis. We assign the above-mentioned two peaks to quasi-LO modes. In theory no quasi-optical phonons can be observed in the configurations $Y(\text{ZZ})\bar{Y}$ and $A(\text{ZZ})Y$ since observable phonons propagate parallel to the XY -plane. In practice, however, phonons whose Z -components of momentum have finite values can also be detected for the following two reasons: the collecting lens has a finite solid angle, and the paths of the incident and scattered light may not be exactly parallel to the XY -plane though we believe that the degree of misalignment is small. Quasi-LO modes in wurtzite structure lie between $A_1(\text{LO})$ and $E_1(\text{LO})$ in frequency. Indeed, the frequencies of the present quasi-LO modes are higher than that of $A_1(\text{LO})$ and a little lower than that of $E_1(\text{LO})$.

The frequency of $E_1(\text{LO})$ in [12] is clearly that of a quasi-LO mode because the propagating direction of the observed phonon in [12] is parallel to $[0\bar{1}1]$, which is parallel neither to the XY -plane nor to the Z -axis. The small difference between the frequency and the pure $E_1(\text{LO})$ frequency is due to the small $A_1(\text{LO})$ – $E_1(\text{LO})$ splitting in GaN.

Using the well known Lyddane–Sachs–Teller (LST) relation, we have also estimated the static dielectric constants, $\epsilon_{\perp 0}$ and $\epsilon_{\parallel 0}$, for GaN. Here $\epsilon_{\perp 0} = \epsilon_{XX} = \epsilon_{YY}$ for the ordinary direction and $\epsilon_{\parallel 0} = \epsilon_{ZZ}$ for the extraordinary one. The values of the LO- and TO-phonon frequencies for A_1 (E_1) given in table 2 have been used for calculating $\epsilon_{\parallel 0}$ ($\epsilon_{\perp 0}$). For the values of the dielectric constants at frequencies much higher than the lattice vibration frequencies, we have assumed isotropic values [7] and used $\epsilon_{\perp \infty} = \epsilon_{\parallel \infty} = 5.35$, as given in [14] and also $\epsilon_{\perp \infty} = \epsilon_{\parallel \infty} = 5.29$ obtained in our own experiments in the infrared region mentioned above. Calculated values are listed in table 3 together with previous results. Note that the discrepancies between the values obtained herein and those in [14] are within a few per cent.

Table 3. Static dielectric constants for wurtzite GaN obtained from the LST relation.

	Static dielectric constant			
	[7]	[14]	Present work	
$\epsilon_{\perp 0}$	12 ± 2	$9.5 \pm 3\%$	9.38^a	9.28^b
$\epsilon_{\parallel 0}$	12 ± 2	$10.4 \pm 3\%$	10.2^a	10.1^b

^a Values calculated using $\epsilon_{\perp \infty} = \epsilon_{\parallel \infty} = 5.35$, given in [14].

^b Values calculated using $\epsilon_{\perp \infty} = \epsilon_{\parallel \infty} = 5.29$; see the text.

In conclusion, we have succeeded in determining all symmetry-allowed optical phonons for GaN by the use of Raman scattering in only one sample. The success is mainly due to the high quality of our sample. We believe that the result for an A_1 (LO) mode frequency, i.e. 735 cm^{-1} , obtained herein terminates a controversy about this mode frequency. The static dielectric constants for GaN have also been estimated.

References

- [1] For a review see, for example, Strite S and Morkoç H 1992 *J. Vac. Sci. Technol.* **B 10** 1237
- [2] Nakamura S, Harada Y and Senoh M 1991 *Appl. Phys. Lett.* **58** 2021
- [3] Nakamura S, Mukai T, Senoh M and Iwasa N 1992 *Japan. J. Appl. Phys.* **31** L139
- [4] Nakamura S and Mukai T 1992 *Japan. J. Appl. Phys.* **31** L1457
- [5] Nakamura S, Senoh M and Mukai T 1993 *Japan. J. Appl. Phys.* **32** L8
- [6] Nakamura S, Mukai T and Senoh M 1994 *Appl. Phys. Lett.* **64** 1687
- [7] Manchon D D Jr, Barker A S Jr, Dean P J and Zetterstrom R B 1970 *Solid State Commun.* **8** 1227
- [8] Lemos V, Argüello C A and Leite R C C 1972 *Solid State Commun.* **11** 1351
- [9] Cingolani A, Ferrara M, Lugarà M and Scamarcio G 1986 *Solid State Commun.* **58** 823
- [10] Kubota K, Kobayashi Y and Fujimoto K 1989 *J. Appl. Phys.* **66** 2984
- [11] Humphreys T P, Sukow C A, Nemanich R J, Posthill J B, Rudder R A, Hattangady S V and Markunas R J 1990 *Mat. Res. Soc. Symp. Proc.* **162** 531
- [12] Hayashi K, Itoh K, Sawaki N and Akasaki I 1991 *Solid State Commun.* **77** 115
- [13] Porto S P S and Krishnan R S 1967 *J. Chem. Phys.* **47** 1009
- [14] Barker A S Jr and Ilegems M 1973 *Phys. Rev. B* **7** 743
- [15] Argüello C A, Rousseau D L and Porto S P S 1969 *Phys. Rev.* **181** 1351